



**HAL**  
open science

## Multispacecraft observations of chorus emissions as a tool for the plasma density fluctuations' remote sensing

Oleksiy Agapitov, Vladimir Krasnoselskikh, Thierry Dudok de Wit, Yuri Khotyaintsev, Jolene Pickett, Ondřej Santolík, Guy Rolland

### ► To cite this version:

Oleksiy Agapitov, Vladimir Krasnoselskikh, Thierry Dudok de Wit, Yuri Khotyaintsev, Jolene Pickett, et al.. Multispacecraft observations of chorus emissions as a tool for the plasma density fluctuations' remote sensing. *Journal of Geophysical Research Space Physics*, 2011, 116, A09222 (12 p.). 10.1029/2011JA016540 . insu-01180062

**HAL Id: insu-01180062**

**<https://insu.hal.science/insu-01180062>**

Submitted on 24 Jul 2015

**HAL** is a multi-disciplinary open access archive for the deposit and dissemination of scientific research documents, whether they are published or not. The documents may come from teaching and research institutions in France or abroad, or from public or private research centers.

L'archive ouverte pluridisciplinaire **HAL**, est destinée au dépôt et à la diffusion de documents scientifiques de niveau recherche, publiés ou non, émanant des établissements d'enseignement et de recherche français ou étrangers, des laboratoires publics ou privés.

## Multispacecraft observations of chorus emissions as a tool for the plasma density fluctuations' remote sensing

Oleksiy Agapitov,<sup>1,2</sup> Vladimir Krasnoselskikh,<sup>1</sup> Thierry Dudok de Wit,<sup>1</sup> Yuri Khotyaintsev,<sup>3</sup> Jolene S. Pickett,<sup>4</sup> Ondřej Santolík,<sup>5,6</sup> and Guy Rolland<sup>7</sup>

Received 8 February 2011; revised 31 May 2011; accepted 9 June 2011; published 21 September 2011.

[1] Discrete ELF/VLF chorus emissions are the most intense electromagnetic plasma waves that are observed in the radiation belts and in the outer magnetosphere of the Earth. They are assumed to propagate approximately along the magnetic field lines and are generated in source regions in the vicinity of the magnetic equator and in minimum  $B$  pockets in the dayside outer zone of the magnetosphere. The presence of plasma density irregularities along the raypath causes a loss of phase coherence of the chorus wave packets. These irregularities are often present around the plasmopause and in the radiation belts; they occur at scales ranging from a few meters up to several hundred kilometers and can be highly anisotropic. Such irregularities result in fluctuations of the dielectric permittivity, whose statistical properties can be studied making use of intersatellite correlations of whistler waves' phases and amplitudes. We demonstrate how the whistler-mode wave properties can be used to infer statistical characteristics of the density fluctuations. The analogy between weakly coupled oscillators under the action of uncorrelated random forces and wave propagation in a randomly fluctuating medium is used to determine the wave phase dependence on the duration of signal recording time. We study chorus whistler-mode waves observed by the Cluster WBD instrument and apply intersatellite correlation analysis to determine the statistical characteristics of the waveform phases and amplitudes. We then infer the statistical characteristics of the plasma density fluctuations and evaluate the spatial distribution of the irregularities using the same chorus events observed by the four Cluster spacecraft.

**Citation:** Agapitov, O., V. Krasnoselskikh, T. Dudok de Wit, Y. Khotyaintsev, J. S. Pickett, O. Santolík, and G. Rolland (2011), Multispacecraft observations of chorus emissions as a tool for the plasma density fluctuations' remote sensing, *J. Geophys. Res.*, 116, A09222, doi:10.1029/2011JA016540.

### 1. Introduction

[2] Discrete ELF/VLF (Extremely Low Frequency/Very Low Frequency) chorus emissions are the most intense electromagnetic plasma waves observed in the radiation belts and in the outer terrestrial \* magnetosphere. These emissions are characterized by rising and falling tones with frequencies ranging from a few hundred Hz to several kHz (see reviews by *Omura et al.* [1991] and *Sazhin and Hayakawa* [1992]). They are important for understanding the dynamics of the

outer radiation belts as they play a crucial role in the acceleration and loss of energetic electrons.

[3] Although ELF/VLF emissions have been intensively studied using data from many different missions (OGO5 [*Burton and Holzer*, 1974], GEOS-1 [*Hayakawa et al.*, 1990], and Plasma Wave Instrument (PWI) aboard GEOTAIL spacecraft [*Nagano et al.*, 1996; *Yagitani et al.* [1999]], analysis of the wave normals and the Poynting fluxes have since shown that these emissions are generated at the geomagnetic equator and propagate to higher latitudes in a nonducted whistler mode [*Burton and Holzer*, 1974; *Hayakawa et al.*, 1990; *Yagitani et al.*, 1999; *Inan et al.*, 2004; *Tsurutani and Smith*, 1974]. Chorus emissions in the radiation belts are believed to be generated through the electron cyclotron instability when the distribution of energetic electrons in the energy range of 5 to 150 keV is strongly anisotropic. Before the Cluster mission, ELF/VLF chorus observations were made by single spacecraft only, except for the observations made simultaneously by ISEE 1 and ISEE 2. By comparing spectrograms from these two spacecraft, *Gurnett et al.* [1979] estimated the characteristic correlation length to be of the order of hundreds of kilometers. These observations, however,

<sup>1</sup>LPC2E/CNRS, Université d'Orléans, Orléans, France.

<sup>2</sup>Astronomy and Space Physics Department, National Taras Shevchenko University of Kiev, Kiev, Ukraine.

<sup>3</sup>Swedish Institute of Space Physics, Uppsala, Sweden.

<sup>4</sup>Department of Physics and Astronomy, University of Iowa, Iowa City, Iowa, USA.

<sup>5</sup>Institute of Atmospheric Physics ASCR, Prague, Czech Republic.

<sup>6</sup>Faculty of Mathematics and Physics, Charles University, Prague, Czech Republic.

<sup>7</sup>CNES, Toulouse, France.

usually did not allow a one-to-one correlation between chorus elements to be carried out.

[4] Recent Poynting flux and polarization measurements by the Cluster spacecraft not only confirmed the location of the source of chorus emissions close to the equatorial plane [Santolik *et al.*, 2005; Parrot *et al.*, 2003] but also showed that the characteristic spatial extent of the chorus source region, measured along the magnetic field lines, should be of the order of 3000–5000 km [Santolik *et al.*, 2004]. The extent of the generation region in the radiation belts was estimated both theoretically [Helliwell, 1965; Trakhtengerts, 1999] and experimentally, using coordinated Cluster observations [Santolik and Gurnett, 2003]. Such estimates, however, are affected both by the characteristic coherence length of the source region and by the effect of whistler-mode wave propagation in an inhomogeneous plasma with random density irregularities. The proper distinction between the two effects is an important issue we address in this paper.

[5] To investigate the position of the source region of chorus emissions, Santolik *et al.* [2004, 2005] used multipoint measurements of the Poynting flux by the STAFF-SA instrument [Cornilleau-Wehrlin *et al.*, 2003] aboard Cluster. These results showed that the central position of the source fluctuates on time scales of minutes within 1000–2000 km of the geomagnetic equatorial plane. Wave planarity estimates were used to characterize the extent of the source region along the field lines and characteristic lengths of the order of several thousands km were found [Santolik *et al.*, 2004, 2005]. The typical macroscopic velocity of the entire source region was determined by averaging the propagation characteristics of several neighboring chorus wave packets and velocities of the order of 100 km/s were found.

[6] With Cluster, the two-point cross-correlation function (hereafter referred to as the correlation function) has become the standard technique for comparing measurements and quantifying the correlation length. For chorus-type whistler-mode waves the correlation was determined by Santolik and Gurnett [2003] using multipoint observations with the Wideband (WBD) instrument [Gurnett *et al.*, 2001] on board Cluster. The Poynting flux measurement for this case has been used to localize the source region in the direction parallel to the magnetic field lines. The correlation coefficient was found to decrease with perpendicular to the background magnetic field separation of the spacecraft. These statistical properties were therefore interpreted by a simple Gaussian model with a perpendicular half-width of 35–60 km for the distribution of power radiated from individual active areas [Santolik and Gurnett, 2003; Santolik *et al.*, 2004].

[7] This characteristic scale of the sources of individual chorus wave packets can be associated either with the characteristic scale of plasma background parameters that will in turn affect the dielectric permittivity tensor of the plasma, or with the characteristic scale of variations in the energetic electron distribution function. The most likely cause for these variations are changes in the plasma density as density irregularities in the magnetosphere are known to play an important role in whistler-mode waves propagation. Evidence for this has been accumulated since the 1950s and 1960s [see, e.g., Sonwalkar, 2006, and refer-

ences therein]. Such irregularities can guide, reflect, and scatter whistler-mode waves and, in general, modify the wave structure. Irregularities have been observed in most magnetospheric regions including the ionosphere, the plasmasphere, the plasmopause, high latitude auroral and polar regions [Carpenter *et al.*, 2002]. Plasma density irregularities can be caused by various processes including plasma instabilities, particle precipitation, and plasma drifts. The dependence of the wave refraction index on the electron density can be used to estimate the averaged electron density. The remote sensing of the magnetospheric plasmas with ground instruments and major discoveries such as the plasmasphere and the plasmopause are based on this property [Carpenter and Anderson, 1992].

[8] Here we investigate the cross-correlation of multipoint wave measurements, assuming that they depend only on the fluctuations of the phase velocity, and we evaluate their characteristic spatial scales. From this we deduce the characteristics of plasma density variations. In contrast to previous studies, we concentrate on the phase information and use the cross-correlation of chorus emissions to assess the spatial scale of density irregularities. The events we consider were observed when the interspacecraft separation of Cluster was small (few tens km), thereby ensuring that all four spacecraft do see the same structures. We assume that the spatial scale of the chorus source transverse to the background magnetic field is about hundred km, i.e. much greater than the chorus wavelength  $\lambda$  ( $\lambda \approx 10$ – $20$  km).

[9] The paper is organized as follows: in section 2 we present a model for wave propagation in an inhomogeneous plasma with random density fluctuations. From this we obtain the model for the correlation function and show how to evaluate in practice the transverse correlation scale of the refraction index and the parallel inhomogeneity. In section 3 the method is applied to Cluster observations. Discussion and Conclusions follow in sections 3 and 4.

## 2. Propagation of Whistler-Mode Waves in a Weakly Inhomogeneous Plasma

### 2.1. Introduction

[10] Now we consider the wave propagation from the source to two spacecraft through the media with random fluctuations of phase velocity. During the propagation, the wave phase  $S$  obtains the random component which depends on the raypath and the amplitude of the phase velocity fluctuations. The direct problem consists in evaluation of the phase and amplitude correlation function dependence on distance to the source and cross-spacecraft distances. The direct problem solution is considered in Appendix A. To evaluate the distance to the wave source and characteristic spatial scales of plasma fluctuations ( $l_{\parallel}$  and  $l_{\perp}$  - correlation scales along and transverse to the magnetic field) one should consider the solution of the inverse problem for a wave propagation from the source to a registration point through a medium with random spatial fluctuations. Let  $u(\vec{r}, t)$  be the wave field (registered by spacecraft at  $\vec{r}$ ) propagating from the source region with unknown location. Plasma is filled up by large scale random density fluctuations with unknown parallel and transverse characteristic scales. Figure 1 illustrates the definition of variables used considering random component of the wave phase difference between the two

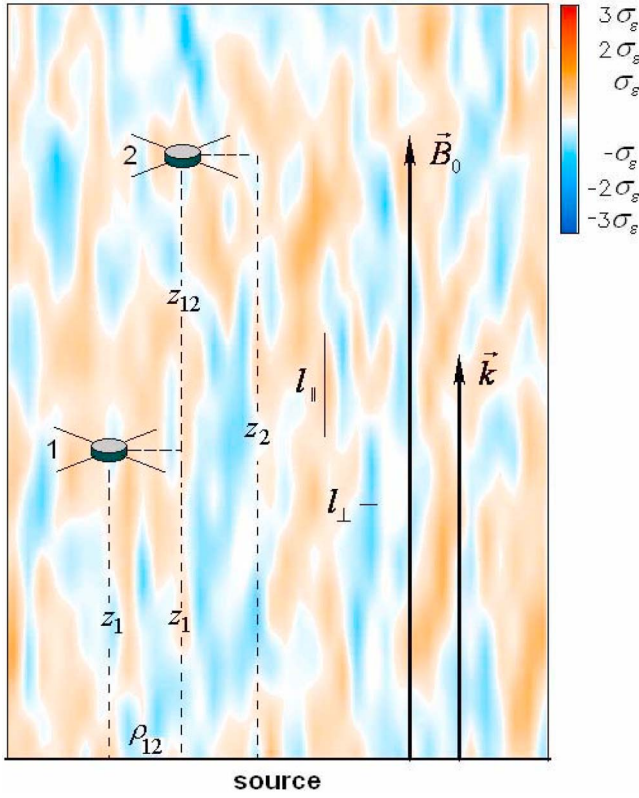


**Figure 1.** Representation of the geometry of the system we consider. Wave measurements are performed aboard two spacecraft shown as cylinders with antennas and situated at  $\vec{r}_1$  and  $\vec{r}_2$ . Segments  $l_{\parallel}$  directed along the magnetic field line and  $l_{\perp}$  are the correlation scales along the magnetic field and transverse to it. The background magnetic field  $\vec{B}_0$  is shown by a long vector directed vertically, as the wave-vector  $\vec{k}$ . The cross-spacecraft distances along and transverse to the wave propagation direction,  $z_{12}$  and  $\rho_{12}$ , are also shown. The distance from the source to the closest spacecraft along the raypath is  $z_1$ . The source is assumed to be placed on the horizontal plane at the bottom.

spacecraft situated at  $\vec{r}_1$  and  $\vec{r}_2$  respectively. Making use of the first-order corrections to the unperturbed solution of the Helmholtz equation (A4) in homogeneous medium one can find the first order perturbations of the wave phase  $S = S_0 + S_1$  and amplitude  $A = A_0 + A_1$ , where indices 0 and 1 correspond to the regular and the random components respectively.

[11] Let us consider the coherence function of the waveform  $u(\vec{r}, t)$  observed at  $\vec{r}_1$  and  $\vec{r}_2$ :

$$\Gamma_u(\vec{r}_1, \vec{r}_2) = \langle u(\vec{r}_1)u^*(\vec{r}_2) \rangle. \quad (1)$$

[12] Neglecting amplitude fluctuations with respect to phase fluctuations (see equation (A14)) the coherence function reads

$$\Gamma_u(\vec{r}_1, \vec{r}_2) \approx |u_0|^2 \langle e^{i[S_1(\vec{r}_1) - S_1(\vec{r}_2)]} \rangle \quad (2)$$

where  $u_0 = A_0 \exp(ikS_0)$ . By means of the relation  $\langle e^{i\xi} \rangle = e^{-\frac{1}{2}\langle \xi^2 \rangle}$  for normally distributed variable  $\xi$  having zero average  $\langle \xi \rangle = 0$ , one obtains the relation

$$\Gamma_u(\vec{r}_1, \vec{r}_2) = I_0 \exp \left[ -\frac{1}{2} D_S(\vec{r}_1, \vec{r}_2) \right], \quad (3)$$

where  $D_S(\vec{r}_1, \vec{r}_2) = \langle (S_1(\vec{r}_1) - S_1(\vec{r}_2))^2 \rangle$  is the phase structure function.

[13] The structure function for the phases can be rewritten as a function of the phase variances  $\sigma_1$  and  $\sigma_2$  at the locations  $\vec{r}_1$  and  $\vec{r}_2$ , then the phase coherence function  $\Gamma_S(\vec{r}_1, \vec{r}_2)$ :

$$D_S(\vec{r}_1, \vec{r}_2) = \sigma_1^2 + \sigma_2^2 - 2\Gamma_S(\vec{r}_1, \vec{r}_2), \quad (4)$$

For the propagation along the local magnetic field (along the  $z$  axis)  $D_{S12}$  can be rewritten in a form (taking into account equation (A11))

$$D_S(\vec{r}_1, \vec{r}_2) = \frac{k^2}{2\langle \varepsilon \rangle} z_1 l_{\parallel} \sigma_{\varepsilon}^2 + \frac{k^2}{2\langle \varepsilon \rangle} z_2 l_{\parallel} \sigma_{\varepsilon}^2 - 2 \frac{k^2}{2\langle \varepsilon \rangle} \sqrt{z_1 z_2} l_{\parallel} \sigma_{\varepsilon}^2 K_S(\vec{r}_1, \vec{r}_2). \quad (5)$$

The phase correlation coefficient here  $K_S(\vec{r}_1, \vec{r}_2) = \Gamma_S(\vec{r}_1, \vec{r}_2) / \sigma_1 \sigma_2$  can be found from equation (A10). Finally, the phase structure function reads

$$D_S(\vec{r}_1, \vec{r}_2) = \frac{k^2}{2\langle \varepsilon \rangle} z_1 l_{\parallel} \sigma_{\varepsilon}^2 \left[ 1 - \exp \left\{ -\frac{\rho_{12}^2}{2l_{\perp}^2} \right\} \right] + \frac{k^2}{2\langle \varepsilon \rangle} z_{12} l_{\parallel} \sigma_{\varepsilon}^2, \quad (6)$$

where  $\rho_1 - \rho_2 = \rho_{12}$ ,  $z_1 - z_2 = z_{12}$ ;  $z_1$  is the distance from the source to the closest spacecraft along the raypath; (Figure 1);  $\varepsilon$  is the dielectric permittivity which can be used in a form A1 for the quasi-parallel propagation;  $\sigma_{\varepsilon}^2$  is the variance of the  $\varepsilon$ .

[14] Up to now we have assumed the stationarity of the electron density fluctuations in the media, neglecting temporal variations of the statistical characteristics due to diffusion, convection, and ordered motions of the plasma. Thus the results obtained can be valid only if the wave propagation time  $t = z/V_{ph}$  is much shorter than the characteristic time of temporal variations of plasma fluctuations,  $\tau \propto \frac{l_{\parallel}}{z} (\frac{v_{\parallel}}{v_{\perp}} + \frac{v_{\perp}}{l_{\perp}})^{-1}$ . This limit is usually called the quasistatic approximation [Tchernov, 1977]. On the other hand, the quasi-stationary statistical characteristics of  $D_S$  can be properly evaluated only on sufficiently long time intervals,  $T \gg \tau$ . For  $T \leq \tau$  the structure function  $D_S(\vec{r}_1, \vec{r}_2)$  is time dependent, thus its estimate  $\tilde{D}_S(\vec{r}_1, \vec{r}_2)$  depends upon the length  $T$  of evaluation time interval and its statistical characteristic parameters. In the limit  $T \ll \tau$  its dependence upon time can be approximated by a linear relation:  $\tilde{D}_S(\vec{r}_1, \vec{r}_2) = \beta D_S(\vec{r}_1, \vec{r}_2) T$ . As a consequence, the estimate of the coherence function  $\tilde{\Gamma}_S(\vec{r}_1, \vec{r}_2)$  becomes also time dependent and it can be presented in a following form

$$\begin{aligned} \tilde{\Gamma}_u(\vec{r}_1, \vec{r}_2) &= \frac{I_0 \gamma}{T} \int_0^T \exp \left[ -\frac{1}{2} (\beta D_S(\vec{r}_1, \vec{r}_2) T') \right] dT' \\ &= I_0 \gamma(\vec{r}_1, \vec{r}_2) \frac{1 - \exp[-(\beta D_S(\vec{r}_1, \vec{r}_2) T)]}{(\beta D_S(\vec{r}_1, \vec{r}_2) T)}. \end{aligned} \quad (7)$$

where  $\gamma(\vec{r}_1, \vec{r}_2) \leq 1$  is time independent parameter that is introduced to account for possible small deviations from Gaussian distribution of fluctuations. Equation (7) is valid for

**Table 1.** Relative Distances of the Cluster Spacecraft Along and Transverse to the Local Magnetic Field on 18 April 2002 for Three Different Time Intervals<sup>a</sup>

sc i—j	$z_{ij}(km)$	$\rho_{ij}(km)$	$\beta D_S(\vec{r}_i, \vec{r}_j)$ 8:46:10	$\beta D_S(\vec{r}_i, \vec{r}_j)$ 8:49:52	$\beta D_S(\vec{r}_i, \vec{r}_j)$ 8:58:29
1—2	188	4	243 ± 6	72 ± 2	78 ± 3
1—3	259.5	72	105 ± 3	196 ± 4	87 ± 1
1—4	119	50	297 ± 5	127 ± 2	67 ± 2
2—3	71.5	69	187 ± 3	144 ± 3	41 ± 1
2—4	68.3	45.5	34 ± 1	41 ± 1	66 ± 2
3—4	139.9	57.2	97 ± 2	132 ± 3	112 ± 3

<sup>a</sup>The obtained distance from the C1 spacecraft to the wave initiation point  $z$  and the characteristic transverse scale of the fluctuations  $\rho$  are listed at the bottom.

$T \ll \tau$ . When  $T$  becomes comparable with  $\tau$ ,  $T \leq \tau$ , the structure function dependence upon time  $\tilde{D}_S(\vec{r}_1, \vec{r}_2)$  becomes close to power law. For  $T \gg \tau$  the coherence function becomes independent of time and takes the form  $I_0 \gamma(\vec{r}_1, \vec{r}_2) \exp[-(\sigma_1^2 + \sigma_2^2 - 2\Gamma_S(\vec{r}_1, \vec{r}_2))]$ . It is worth noting that if  $z \gg l_{\parallel}$  the structure function dependence upon the time  $\tilde{D}_S(\vec{r}_1, \vec{r}_2)$  is close to power law for all  $T$  because  $\tau \propto \frac{l_{\parallel}}{z}$  and  $T$  is supposed to be larger than the time that wave propagates from the source to observer. Thus the technique proposed here can be applicable only when  $z \sim l_{\parallel}$ .

## 2.2. Application to the Spacecraft Measurements

[15] Let's rewrite the equation (6) introducing explicitly the variable  $z_{\min}$  – distance from the wave source to the nearest spacecraft, and  $\alpha = \frac{k^2}{2(\epsilon)} \beta l_{\parallel} \sigma_{\epsilon}^2$ . Equation (6) then reads

$$\beta D_S(\vec{r}_1, \vec{r}_2) = \alpha \left[ z_{\min} \left( 1 - \exp\left(-\frac{\rho_{12}^2}{2l_{\perp}^2}\right) \right) + 0.5z_{12} \right]. \quad (8)$$

[16] The combination  $\beta D_S(\vec{r}_1, \vec{r}_2)$  can be estimated making use of multispacecraft data. Assuming that the statistics of fluctuations is Gaussian, thus the time dependence of the

coherence function is described by expression (7) one can find by means of the least square technique  $\beta D_S(\vec{r}_1, \vec{r}_2)$ . It is necessary to have measurements in three points to find out  $z_{\min}$ ,  $\alpha$  and  $l_{\perp}$  for quasi-parallel wave propagation. In the case of four-point Cluster measurements we have six equations; thus the system of equations for quasi-parallel wave propagation is overdetermined. This system can be solved by means of the quadratic form minimization

$$R(\alpha, l_{\perp}, z_{\min}) = \sum_{i,j,i \neq j} \left( 1 - \frac{D_{ij}(\alpha, l_{\perp}, z_{\min})}{D_{ij}} \right)^2. \quad (9)$$

[17] Considering  $R(\alpha, l_{\perp}, z_{\min})$  as a functional over variables  $\alpha$ ,  $l_{\perp}$ , and  $z_{\min}$ , one gets the system of equations following from three relations:

$$\frac{\partial R(\alpha, l_{\perp}, z_{\min})}{\partial \alpha} = 0; \quad \frac{\partial R(\alpha, l_{\perp}, z_{\min})}{\partial l_{\perp}} = 0; \quad \frac{\partial R(\alpha, l_{\perp}, z_{\min})}{\partial z} = 0, \quad (10)$$

which can be solved numerically using a most rapid gradient technique [Dennis and Schabel, 1983]. In the next section we apply it to the multipoint measurements of the waveforms of electric field aboard Cluster spacecraft.

## 3. Cross-Correlation Data Analysis Results

[18] Now we shall apply above described technique to analyze the multipoint Cluster measurements of the electric field waveforms registered by the Wide-Band Data (WBD) plasma wave instrument [Gurnett et al., 2001]. The Cluster WBD plasma wave receiver is designed to provide high-resolution measurements of both electric and magnetic fields in selected frequency bands from 25 Hz to 577 kHz as part of the Cluster Wave Experiment Consortium (WEC). The WBD data are obtained along only one axis in one of three

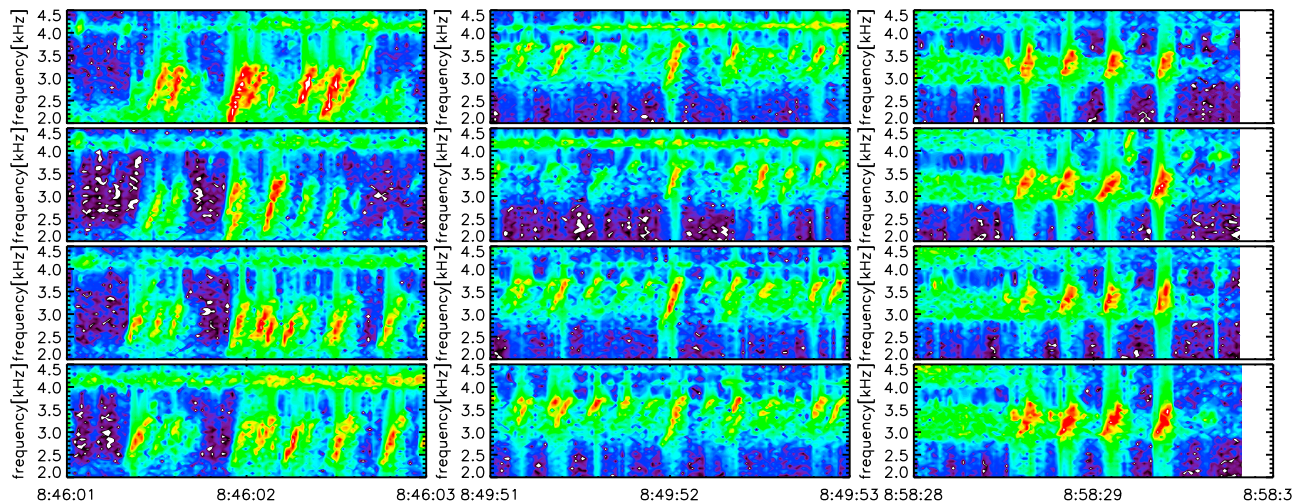


**Figure 2.** Time-frequency power spectrograms of the electric field fluctuations captured by the WBD instruments aboard the four Cluster spacecraft on 18 April 2002. (top to bottom) Data from C1, C2, C3, and C4 respectively.

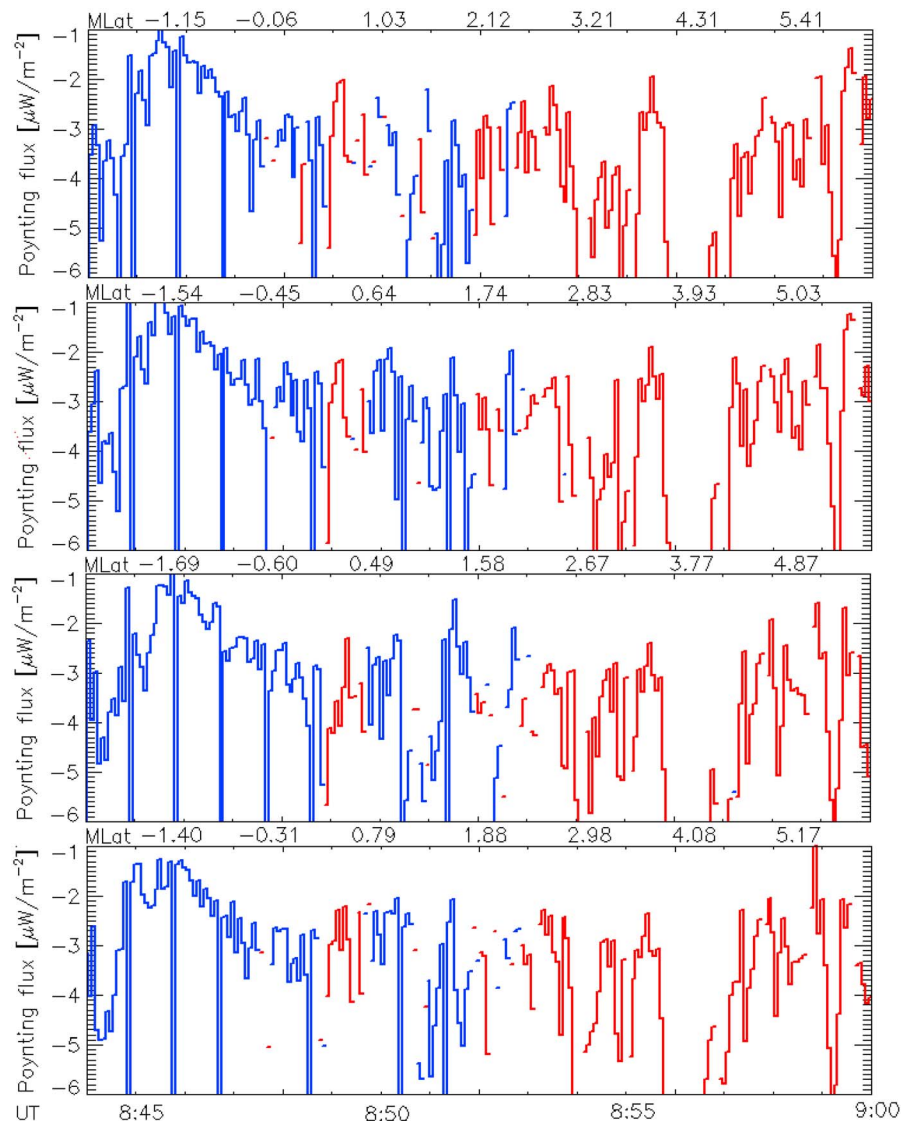


**Figure 3.** Poynting flux along the background magnetic field in the frequency range 3–4 kHz. The red and blue colors shows the flux direction along and opposite to the background magnetic field, respectively. (top to bottom) Data from C1, C2, C3, and C4, respectively.

filter bandwidth modes: 9.5 kHz, 19 kHz, 77 kHz. In the current work the continuous waveforms of the electric field variations were used for detailed high-resolution correlation analysis. Our analysis of the wave polarization properties is primarily based on data from the Spatio-Temporal Analysis of Field Fluctuations–Spectrum Analyzer (STAFF-SA) experiment [Cornilleau-Wehrlin *et al.*, 2003]. It calculates the complete spectral matrix (real and imaginary part) of the three magnetic components measured by the STAFF search coil magnetometer and the two electric field components from the EFW experiment [Gustafsson *et al.*, 2001]. The spectral matrix is computed on board for 27 frequency channels which are logarithmically spaced between 8.8 Hz and 3.56 kHz. We analyze discrete large amplitude chorus-type emissions observed during perigee passes of the Cluster spacecraft on 18 April 2002 during the recovery phase of the magnetic storm (the  $D_{st}$  index decreased to  $-126$  nT at

08:00 UT and to  $-116$  nT at 09:00 UT; the  $K_p$  index value was equal to 6– during the event). For these passes the Cluster spacecraft were located near the geomagnetic equator on the night side (MLT of 21:00) at a radial distance near  $4.4 R_E$ . The four spacecraft were located very close to each other, with maximum separation 260 km along  $B$  and less than 100 km in the perpendicular to  $B$  direction (see Table 1). Intense chorus emissions were observed between 08:20 and 09:30 UT by the WBD plasma wave instruments and by the STAFF-SA spectral analyzers. During this time interval the WBD instruments were set up to measure continuously electric field waveforms with the pass band filters between 50 Hz and 9.5 kHz and a sampling frequency 27.44 kHz. This data set was previously analyzed by Santolik and Gurnett [2003], and Santolik *et al.* [2004] in order to determine the spatial extent of the chorus source region by means of cross-correlation analysis of

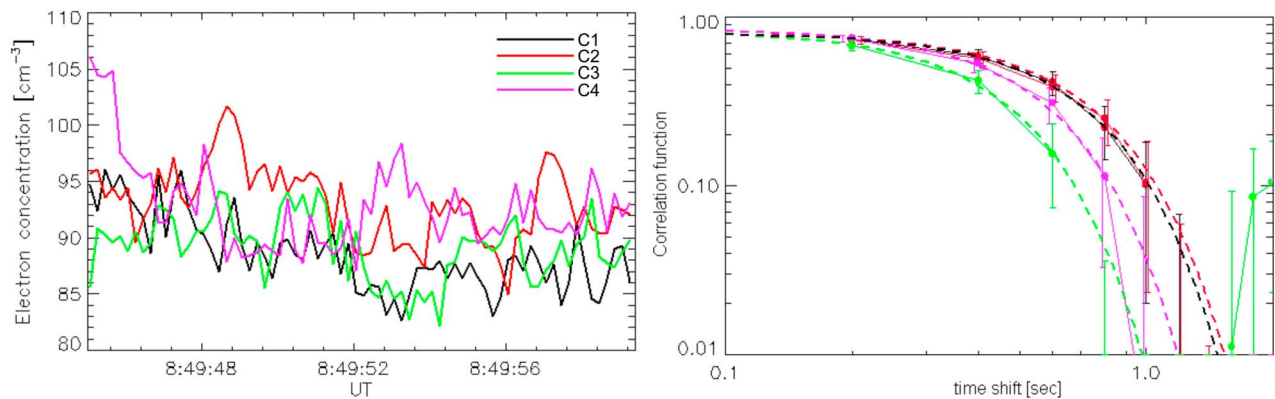


**Figure 4.** (left) Density estimate based on EFW electric potential measurements aboard the Cluster spacecraft. The four traces correspond to each of the spacecraft using the conventional Cluster colors (C1, black; C2, red; C3, green; and C4, magenta). (right) The autocorrelation function of the density fluctuations. The estimates obtained by assuming a Gaussian distribution are shown with dashed lines (colors are the same as for Figure 4, left).

averaged amplitudes of the electric field waveforms observed on different spacecraft. The same data set was analyzed by *Inan et al.* [2004], who found a relatively small frequency difference between the waves observed aboard different spacecraft.

[19] The time-frequency spectrograms of three time intervals we choose for this study are shown in Figure 2. First we investigate the Poynting vector direction using STAFF-SA spectral matrices. The wave vector directions are found to be very close to the local magnetic field direction. The Poynting vector projection along the background magnetic field obtained for the four Cluster spacecraft is shown in Figure 3. During the magnetic equator crossing at 8:48–8:52 UT the direction of the Poynting vector changes which is consistent with the position of the wave source region in the vicinity of the geomagnetic equator. The observed dynamic behavior of the Poynting flux indicates the change of the source location which can be caused by large amplitude disturbances of the magnetic field magnitude near the geomagnetic equator.

[20] Waves propagating from the source are affected by plasma density and magnetic field fluctuations. However the amplitude of B fluctuations is much smaller, and thus their contribution can be neglected. In order to characterize these fluctuations we use the plasma floating potential measurements by EFW instrument from which we infer plasma density variations [*Gustafsson et al.*, 2001; *Khotyainsev et al.*, 2010] at the rate of 5 samples per second shown in Figure 4. The spacecraft potential measurements are converted into the plasma density using an empirical model described by *Gustafsson et al.* [2001] and *Pedersen et al.* [2008]. To obtain absolute values of density fluctuations these measurements are calibrated using absolute electron density measured by means of active sounding and passive measurements of the WHISPER experiment (Waves of High Frequency and Sounder for Probing of Electron Density by Relaxation). It consists of a pulse transmitter in the frequency range 4–80 kHz, a wave receiver (2–80 kHz) and a wave spectrum analyzer [*Décroux et al.*, 2001]. We find that the plasma

density fluctuation statistics is close to Gaussian with the average amplitude of fluctuations being about 5% from the background plasma density and the characteristic time scale of fluctuations  $\tau$  being about 0.5 sec (see Figure 4). The corresponding spatial scale of density fluctuation is estimated by use of plasma flow velocity determined by CIS (the Cluster Ion Spectrometry experiment measures the full, three-dimensional ion distribution of the major magnetospheric ions from the thermal energies to about 40 keV/e [*Rème et al.*, 2001]) instrument and found to be about 70–90 km transverse and 900–1500 km along the background magnetic field.

[21] Next we carry out the study of the cross-correlations between electric field waveforms measured aboard different spacecraft (shown in Figure 5). We compare the observed cross-correlation coefficients with two different functions: the functional time dependence corresponding to expression obtained in section 2, equation (7), blue solid line, and with the power law dependence, solid red line. The power law dependence with the index-1/2 corresponds to the absence of phase correlation as it was discussed in section 2. The best agreement is found for the first fit corresponding to equation (7).

[22] The structure function values obtained from fitting of the cross-correlation coefficients by equation (7) (blue line in Figure 5) are shown in Table 1 for all three time intervals. The structure function is then used to infer the correlation lengths of the dielectric permittivity fluctuations in the plasma. A good agreement with the fit corresponding to expression (7) allows one to solve numerically the system of equations (10) to obtain estimates for the distance from the spacecraft to the wave source  $z$  and the electron density fluctuation spatial characteristic scale  $l_{\perp}$ . For the three time intervals analyzed the following results were obtained:  $l_{\perp} = 80 \pm 10$  km and  $z = 1400 \pm 200$  km (8:46:01–8:46:03 UT),  $l_{\perp} = 75 \pm 10$  km and  $z = -800 \pm 120$  km (8:49:51–8:49:53 UT, shown in Figure 5);  $l_{\perp} = 90 \pm 10$  km and  $z = 320 \pm 50$  km (8:58:28–8:58:30 UT). These  $z$  values correspond to displacement of the wave source from the magnetic equator

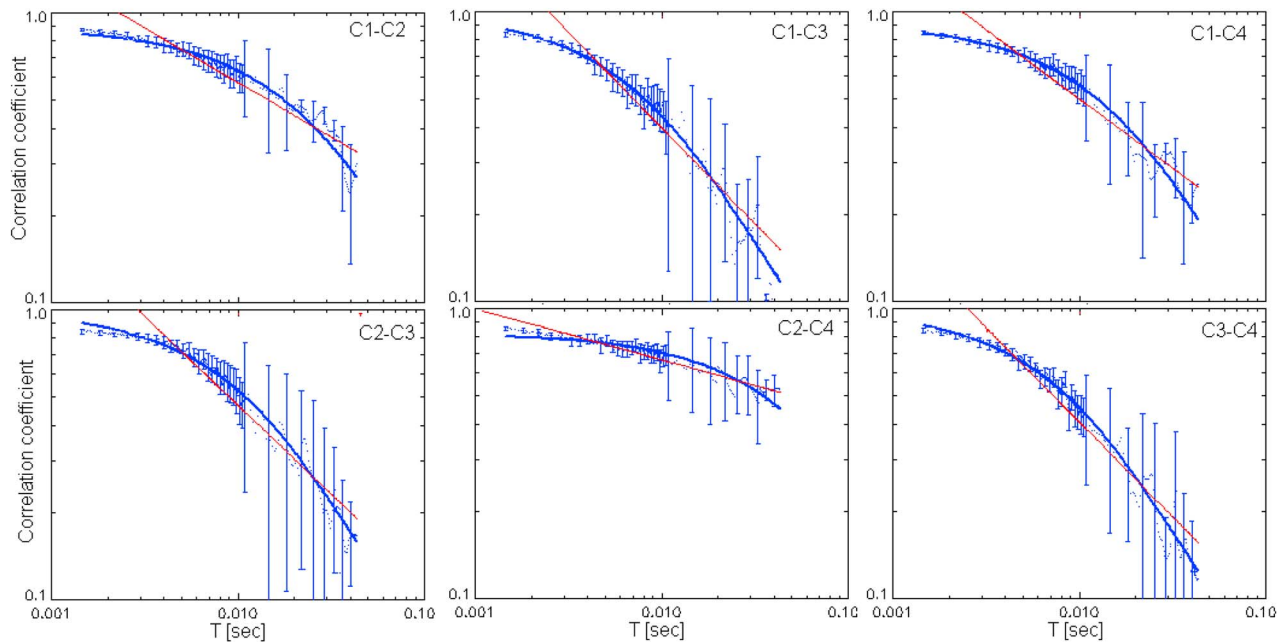


**Figure 5.** Cross-correlation analysis of the discrete chorus element observed at 08:49:52 UT on 18 April 2002 aboard the four Cluster spacecraft. The correlation coefficient time dependence is shown for spacecraft pairs 1–2, 1–3, 1–4, 2–3, 2–4, and 3–4, respectively. The approximation with the  $\frac{(1 - \exp(-D_s T / \beta))}{D_s T / \beta}$  function is shown with a solid blue line. The approximation with the power law dependence is shown with a red dashed line.

about 400 km,  $-850$  km and 1600 km respectively. These estimated positions are in a good agreement with the Poynting vector direction finding presented in Figure 3.

#### 4. Discussion

[23] The cross-correlation dependencies upon the time between chorus waveforms registered aboard separate spacecraft for the three time intervals presented above are well described by the model developed in section 2. It is based on the solution of the simplified problem describing statistical properties of phase cross-correlations for wave propagation through the system with random fluctuations of the phase velocity.

[24] Two spatial scales affect the wave correlation characteristics during the propagation through the media with random electron density fluctuations: the density fluctuations characteristic scale and the distance from the source. We estimate the transverse coherence scale of the chorus waves generation region on the basis of simultaneous multispacecraft measurements of the same chorus elements obtained by Cluster during 2002–2003. We found this scale to be  $\sim 600$  km for the  $L$ -shell about 4–5. For larger transverse distances the individual chorus elements are not detected simultaneously by two spacecraft. This confirms the measurements by ISEE-1, 2 who discovered that the characteristic correlation length is of the order of hundreds of kilometers [Gurnett *et al.*, 1979]. For the outer magnetosphere (for  $L$ -shell about 8–9) the transverse coherence scale was found to be about 300 kilometers [Agapitov *et al.*, 2010]. The characteristic perpendicular correlation scale we find here is significantly shorter  $\sim 60$  km. We found that the

observed phase and amplitude correlation properties can be explained in terms of wave propagation effects caused by random fluctuations of the wave phase velocity related to density fluctuations.

[25] The solution of the system of equations (7) for the parameters obtained by Cluster spacecraft (listed in Table 1) gives the fluctuation spatial scales,  $l_{\perp}$ , in a range of 60–90 km (the ion gyroradius radius is about 25–30 km). This is in good agreement with the direct evaluation of the plasma density variations correlation length obtained using EFW direct measurements of the electron density fluctuations and CIS measurements of the plasma flow velocity. It is worth mentioning here that in the outer magnetosphere it was found that the fluctuation scale is also of the order of the ion gyroradius [Agapitov *et al.*, 2010]. On the basis of the correlation analysis of the amplitude we find the characteristic correlation length in a range 40–60 km (according to equation (A12)). This result is in good agreement with the results obtained by Santolik and Gurnett [2003] and Santolik *et al.* [2004] who used the correlation analysis of the amplitudes of the Fourier components. The characteristic scale of the inhomogeneity along the background magnetic field,  $l_{\parallel}$ , is estimated using the ratio between plasma velocity components along the magnetic field and transverse to it.  $l_{\parallel}$  is found to be in a range 1000–1500 km, which is of the same order as the characteristic thickness of the source (3000–5000 km) found in previous studies [Santolik and Gurnett, 2003; Santolik *et al.*, 2004]. We find here the lengths of the raypath,  $z$ , in the range of 300–1000 km that is sufficiently smaller than the characteristic thickness

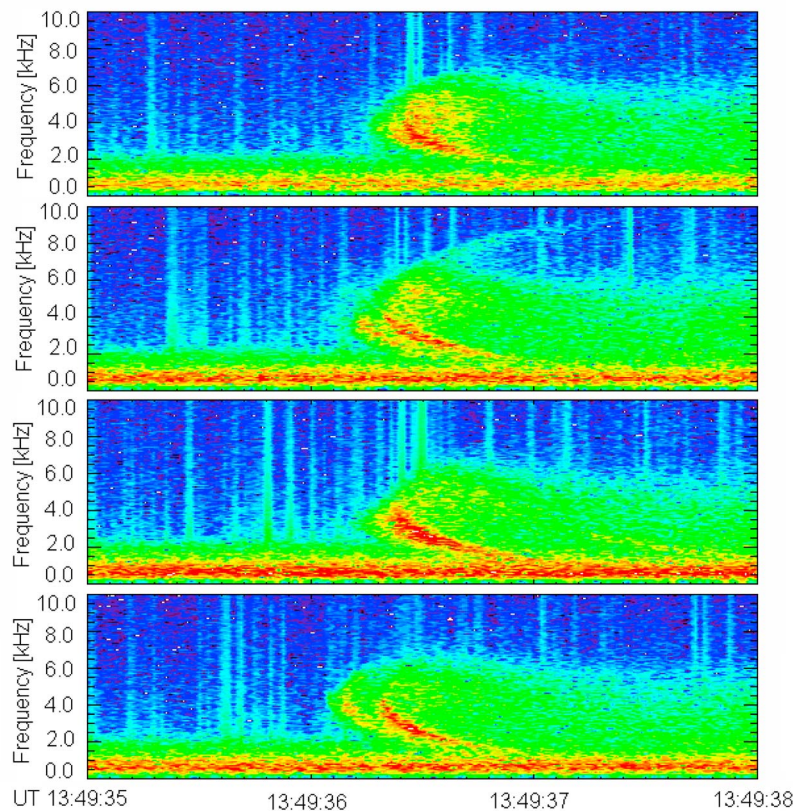


**Figure 6.** The dynamic time–frequency spectrograms of the WBD electric field measurements on 2001-02-04, 13:49:35–13:49:38 UT. (top to bottom) Data from C1, C2, C3, and C4, respectively.

of the active zone of the source. Thus one should conclude that the characteristic scales we found can be the characteristic scales of inhomogeneities directly in the source region.

[26] Velocity of a moving wave source, if it is significantly large, can be estimated from the correlation analysis of close wave packets or of the different parts of the same wave packet. This was done for example by *Agapitov et al.* [2010] using THEMIS VLF measurements. For the presented events the estimated source velocity was small, i.e. of the order of evaluation errors, and as a result the averaged source position is presented.

[27] The technique proposed can also be applied to the waves propagating obliquely to the magnetic field. In such a case the scale  $l_{\parallel}$  appears explicitly in equation (6). To solve the system of equations (10) four point measurements are necessary, thus the Cluster spacecraft provide sufficient number of satellites to perform such an analysis. However, for the chorus waves in the vicinity of the magnetic equator (where the angles between the wave-vector and background magnetic field are less than  $30^{\circ}$ ) the wave propagation can be considered as quasi-parallel with sufficient accuracy. Indeed, for the events presented the angles between the wave-vector and the background magnetic field are less than  $20^{\circ}$ .

[28] Finally, we should check whether our initial assumptions of the applicability of the geometrical optic approximation are justified. The time of the observed

whistler wave propagation from the source to spacecraft can be estimated to be about 0.01 sec (group velocity is estimated from the equation (A1), it is found to be about 0.1 of the speed of light). The characteristic temporal scale of the electron density fluctuations from EWF measurements is about 0.3–0.5 sec. Thus the quasi-static assumption for the whistler wave propagation is satisfied. The size of the first Fresnel zone,  $\sqrt{z\lambda}$  (where  $\lambda \sim 4\text{--}6$  km is a wave length) is less than the characteristic inhomogeneity scale  $l_{\perp}$ , thus, the diffraction effects are negligible (equation (A9)). The relation for wavelength  $\lambda \ll l_{\parallel}$  is satisfied with a good margin for the obtained characteristic scales. Thus the geometrical optics approximation, as discussed in Appendix A, is applicable. The perturbation technique applied to the wave propagation is applicable for the fluctuations level  $\delta n \ll n$ , which is certainly true in our case.

[29] However the proposed technique can not be applied for the cases when the distance to the source is much greater than the parallel fluctuation scale  $z \gg l_{\parallel}$ . As we have shown in section 2 in this case the phase coherence will be lost. As an example we present an event with different correlation properties, whistler generated in the atmosphere. The time-frequency spectrograms of the waveforms registered by Cluster WBD instrument during the time interval from 13:49:35 to 13:49:38 UT, 4 February 2001 are shown in Figure 6. The same discrete whistler wave packet is detected aboard the four Cluster spacecraft and the similar time-frequency properties of the wave power are observed. The

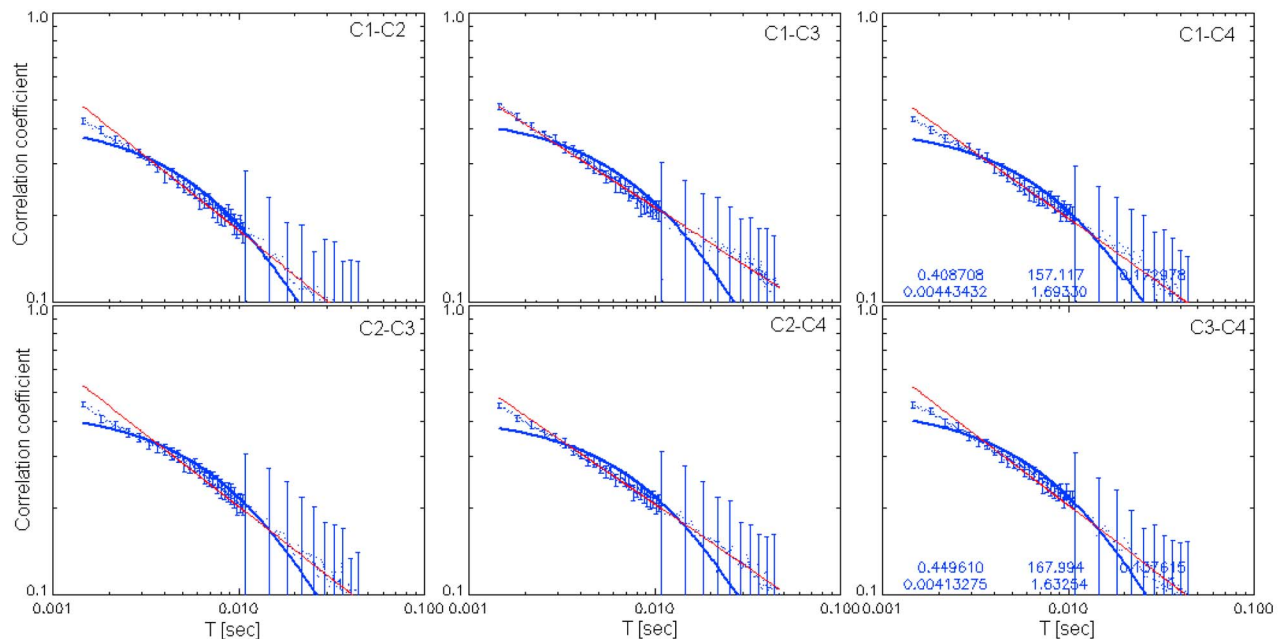


**Figure 7.** The phase cross-correlation dependence on estimation time for the discrete whistler wave packets observed on 2001-02-04, 13:49:35–13:49:38 UT, aboard the Cluster spacecraft. The approximations shown are the same as in Figure 5.

correlation functions for the different Cluster spacecraft pairs are shown in Figure 7. The time dependencies are best fitted by the power law, that shows that  $z \gg l_{\parallel}$  and the phase coherence is absent.

## 5. Conclusions

[30] Random inhomogeneities of plasma density are found to have a strong effect on the propagation of whistler-mode waves resulting in fluctuations of the phase velocity of the waves. Irregularities of the phase velocity along the raypath may lead to loss of the phase coherence of the wave packet. Based on the intersatellite cross-correlation analysis of whistler-mode wave phases and amplitudes we performed the study of the statistical characteristics of the fluctuations of the refraction index of in the plasma. From such cross-correlation analysis we reconstruct the properties of the density fluctuations along the wave propagation path. This allows us to distinguish the wave source properties from the effects of the wave propagation through the media. We study chorus waves in the vicinity of the magnetic equator (for magnetic latitudes  $<20^{\circ}$  and  $L$ -shells less than 6) having angles with the magnetic field less than  $30^{\circ}$ . In this case the wave propagation can be considered as quasi-parallel. The wave propagation is analyzed in a frame of the geometric optics approximation for cold plasma. The cold plasma approximation is well justified for the observed  $\beta \ll 1$ . The obtained spatial fluctuation scales ( $l_{\parallel}$  and  $l_{\perp}$ ) justify the use of the geometric optics approximation ( $\lambda \ll l_{\parallel}$  and  $\sqrt{z\lambda} < l_{\perp}$ ). The proposed technique can be applied to VLF wave form measurements in a case if the same wave packet is observed aboard three or more spacecraft; the variance of the density is much less than the unperturbed value, temporal scale of fluctuations is greater than

the wave period and of the same order with the wave packet duration; distance from the source to the spacecraft is of the same order with the fluctuation spatial scale parallel to the background magnetic field.

[31] The proposed analysis technique for the quasi-parallel wave propagation was applied to the Cluster WBD measurements of the electric field in the chorus generation region and the following results are obtained:

[32] 1. The characteristic spatial scales of plasma density irregularities transverse to the local magnetic field are found to be in a range from 60 to 110 km, which is of the order of the local ion gyroradius. We find that the chorus wave phase correlation scale is defined by the density fluctuations scale but not by the size of the source near the generation region.

[33] 2. The obtained locations of the wave sources are found to be in a good agreement with positions estimated from the multipoint Poynting flux measurements. The obtained distances from spacecraft to the wave source (from 300 to 1000 km) are sufficiently smaller than the characteristic thickness of the source region, which is known from previous studies to be of the order of 3000–5000 km. Thus the estimated parallel fluctuation scale corresponds to the characteristic scale of the inhomogeneities of the source.

[34] This analysis shows that whistler-mode waves can be used as a tool for remote sensing of statistical characteristics of the electron density fluctuations.

## Appendix A

[35] To consider the properties of the chorus wave propagation in magnetized plasmas with random density fluctuations we start from the propagation properties of chorus waves, which belong to the whistler wave mode. We consider the so-called electron whistler-mode waves in the

frequency range  $\omega_{LH} < \omega < \Omega_e$  (where  $\omega_{LH}$  is the lower hybrid frequency, and  $\Omega_e = |e|B/m_e$  is the electron gyrofrequency) which propagate almost parallel to the magnetic field. The refraction index can be found by using the dispersion relation for quasiparallel propagation in the cold plasma approximation [Helliwell, 1965]:

$$\varepsilon(\omega, \theta) = 1 + \frac{\omega_{pe}^2}{\omega(\Omega_e |\cos \theta| - \omega)}, \quad (\text{A1})$$

where  $\omega_{pe}$  is the electron plasma frequency and  $\theta$  is the angle between the wave  $k$ -vector and the background magnetic field. Dependence upon the angle results in anisotropy of the phase and group velocities, and dependence of the wave polarization upon the angle.

[36] In magnetized plasmas the effect of density fluctuations is anisotropic; in the simplest case they can be described by two characteristic correlation lengths: parallel and perpendicular to the magnetic field. Density inhomogeneities can be separated into two classes depending on their characteristic scale with respect to the wavelength of waves. Small scale inhomogeneities can scatter whistler-mode waves in all directions and thus profoundly change their characteristics. Large scale inhomogeneities with spatial scales larger than the whistler-mode wavelength result in slow variation of the wave  $k$ -vector amplitude and direction of propagation.

[37] Let us consider a wave propagating from the source region in a plasma with large scale random density fluctuations characterized by two characteristic scales  $l_{\parallel}$  and  $l_{\perp}$  parallel and perpendicular to the background magnetic field respectively. As we are not interested in variations of the wave polarization, for the sake of simplicity we apply the perturbation technique and consider a scalar field model

$$u(\vec{r}, t) = A_0 \exp\{iS + \chi\}, \quad (\text{A2})$$

where  $u(\vec{r}, t)$  is the field perturbation at the detection point,  $S$  is the wave phase, and  $\chi \equiv \ln(A/A_0)$  is the wave amplitude level,  $A_0$  and  $A$  are wave amplitudes in the source and at the detector, respectively.

[38] We assume that the wave propagation can be described in the Geometrical Optics Approximation (GOA), which means that  $l_{\parallel}, l_{\perp} \gg \lambda$ , where  $\lambda$  is the wavelength. Without loss of generality the  $z$ -axis is directed along the background magnetic field,  $\vec{\rho}$  is perpendicular to it, and the distribution in the perpendicular direction is isotropic. Let us also assume the correlation function of the permittivity constant  $\Psi_{\varepsilon}(\vec{r}) = \langle \varepsilon(\vec{r}') \varepsilon(\vec{r}' + \vec{r}) \rangle$  (where  $\langle \dots \rangle$  means the ensemble averaging) to be described by an anisotropic Gaussian:

$$\Psi_{\varepsilon}(\vec{r}) = \sigma_{\varepsilon}^2 \exp\left[-\frac{z^2}{2l_{\parallel}^2} - \frac{x^2 + y^2}{2l_{\perp}^2}\right], \quad (\text{A3})$$

[39] The primary wave is supposed to propagate along the magnetic field. The amplitude level fluctuations  $\chi$  can be evaluated from the Helmholtz equation

$$\Delta u + k^2 \varepsilon(\vec{r}) u = 0. \quad (\text{A4})$$

[40] For small amplitude  $\varepsilon$  fluctuations the wave perturbation wave amplitude  $A$  and phase gradient  $\nabla S$  are the

weak dependence coordinate functions (in a scale of the wavelength  $\lambda$ ). Following Rytov *et al.* [1978] and taking into account the weak dependence of  $A$  and  $\nabla S$  using the decomposition of the amplitude to subset of the wave number power  $A = A_0 + A_1 + \dots$ , where  $A_0 \gg A_1$  etc. Using  $S = \varphi \cdot k$  (where  $\varphi$  is an eikonal) after substitution in (A4) one gets the system of equations for  $\varphi$  and for the decomposition coefficients  $A_0, A_1, \dots$ . The equation for the eikonal  $\varphi$  is

$$(\nabla \varphi)^2 = \varepsilon. \quad (\text{A5})$$

[41] The solutions of the eikonal equation (A5) correspond to a raypath with the minimal value of functional  $\int \sqrt{\varepsilon} ds$ , the Fermat principle. In the case of a known raypath (techniques for the raypath determination are discussed by Tchernov [1977]) equation (A5) can be integrated along the raypath and the eikonal can be written as

$$\varphi = \int^s \sqrt{\varepsilon(\vec{r}(s))} ds \quad (\text{A6})$$

[42] In a media with random fluctuations equation (A6) can be solved using the perturbation technique. Let  $\varepsilon(\vec{r}) = \langle \varepsilon(\vec{r}) \rangle + \tilde{\varepsilon}(\vec{r})$  with the random part  $\tilde{\varepsilon}(\langle \tilde{\varepsilon} \rangle = 0, \langle \tilde{\varepsilon}^2 \rangle = \sigma_{\varepsilon}^2)$ . The random part is supposed to be much smaller than the regular one:  $\sigma_{\varepsilon} \ll \langle \varepsilon \rangle$ . Let us consider the eikonal as the series  $\varphi = \varphi_0 + \varphi_1 + \dots$  ( $\varphi \gg \varphi_0 \gg \varphi_1 \gg \dots$ ), where  $\varphi_0$  is supposed to be a solution of the unperturbed eikonal equation

$$(\nabla \varphi_0)^2 = \langle \varepsilon \rangle. \quad (\text{A7})$$

[43] Let us further consider the eikonal subject to the first expansion term  $\varphi \approx \varphi_0 + \varphi_1$ . In the simplest case of a plane wave propagating along the  $z$  axis (along the background magnetic field) the unperturbed eikonal value is  $\varphi_0 = \sqrt{\langle \varepsilon \rangle} z$ . The ray paths are straight lines parallel to the  $z$  axis. The eikonal perturbation value is  $\varphi_1$

$$\varphi_1 = \frac{1}{2\sqrt{\langle \varepsilon \rangle}} \int_0^z \tilde{\varepsilon}(x, y, z') dz' \quad (\text{A8})$$

where  $\langle \varphi_1 \rangle = 0$  and for the Gaussian statistics of the fluctuations of the  $\varepsilon$ ,  $\varphi_1$  is Gaussian also. The applicability of GOA is justified if the first Fresnel zone is much smaller than the characteristic inhomogeneity scale of the dielectric permittivity:

$$\sqrt{\lambda z} \ll l_{\parallel}, l_{\perp}, \quad (\text{A9})$$

[44] Here,  $z$  is the raypath length. The phase and propagation direction of the fluctuations (but not the amplitude level) can be processed using the GOA beyond the bounds of the first Fresnel zone. We check in section 4 (Discussion) whether the conditions of applicability are met.

[45] Now we consider the wave propagation along the  $z$ -axis. For a Gaussian correlation function  $\varepsilon$  with two characteristic scales, parallel and perpendicular, the eikonal correlation function at the points  $\vec{r}_1$  and  $\vec{r}_2$  can be written as [Rytov *et al.*, 1978]:

$$\Psi_S(\vec{r}_1, \vec{r}_2) = \sqrt{\frac{\pi z_{\min} l_{\parallel} k^2 \sigma_{\varepsilon}^2}{2 \langle \varepsilon(\vec{r}) \rangle}} \exp\left[-\frac{(\vec{\rho}_1 - \vec{\rho}_2)^2}{2l_{\perp}^2}\right], \quad (\text{A10})$$

where  $\vec{k}$  is the wave number, the vectors  $\vec{r}_i$  are written in a form of longitudinal  $z_i$  and transversal  $\vec{\rho}_i$  to the background magnetic field components (fluctuations and wave observation parameters are shown schematically in Figure 1);  $z_{\min}$  is the minimal from  $z_1$  and  $z_2$  distances from the source. Due to the spatial statistic homogeneity of the fluctuations the correlation function depends on the difference  $(\vec{\rho}_1 - \vec{\rho}_2)^2$ . It then follows for the wave phase variance

$$\sigma_S^2(z) = \sqrt{\frac{\pi z l_{\parallel} k^2 \sigma_{\epsilon}^2}{2 \cdot 2 \langle \epsilon(\vec{r}) \rangle}}. \quad (\text{A11})$$

[46] Note that the phase variance is proportional to the raypath length, to the variance of the dielectric permittivity  $\sigma_{\epsilon}^2$ , and to the effective parallel correlation length  $l_{\parallel}$ . Another important characteristic we are interested in is the correlation function of the amplitude. Using the same approximation, we have

$$\Psi_{\chi}(\vec{\rho}, z) = \sqrt{\frac{\pi l_{\parallel} z^3}{2 l_{\perp}^4}} \frac{\sigma_{\epsilon}^2}{3 \langle \epsilon \rangle} \left( \frac{\rho^4}{8 l_{\perp}^4} - \frac{\rho^2}{l_{\perp}^2} + 1 \right) \exp\left(-\frac{\rho^2}{2 l_{\perp}^2}\right), \quad (\text{A12})$$

and using it the expression for the variance of the amplitude becomes

$$\sigma_{\chi}^2 = \frac{\sqrt{2\pi} z^3 l_{\parallel}}{3 \langle \epsilon \rangle l_{\perp}^4} \sigma_{\epsilon}^2. \quad (\text{A13})$$

Equations (A12) and (A13) are the modifications of the relation obtained by Rytov *et al.* [1978] for the case of different parallel  $l_{\parallel}$  and transverse  $l_{\perp}$  scales. This variance is proportional to the 3rd degree of the raypath length in the GOA. By comparing the variance of the amplitude and the eikonal one finds

$$\sigma_{\chi}^2 / \sigma_S^2 = \frac{4z^2}{3 l_{\perp}^4 k^2}, \quad (\text{A14})$$

From this we expect the variance of the amplitude to be significantly smaller than that of the eikonal. The GOA is applicable when  $z\lambda \ll l_{\perp}^2$ . For the regions of GOA validity condition (A9) is valid: the size of the first Fresnel zone is much smaller than the  $\epsilon$  fluctuation characteristic scale  $l_{\perp}$  and  $l_{\parallel}$ . Thus for GOA validity the amplitude level fluctuations variance is much less than the phase fluctuations variance  $\sigma_{\chi}^2 \gg \sigma_S^2 = k^2 \sigma_{\varphi}^2$ . Therefore, the amplitude level fluctuations can be neglected in comparison with the phase fluctuations.

[47] **Acknowledgments.** This work was financially supported by CNES through the grant “Modèles d’ondes” and by the ECO NET programme of EGIDE (France). J.S.P. acknowledges support from NASA Goddard Space Flight Center under grant NX07AI24G. The authors are thankful to F. Lefeuvre and Y. Zaliznyak for helpful discussions. The research of Y.K. is supported by the Swedish Research Council, grant 2007-4377. O.S. acknowledges support from grants GACR P205-10-2279, ME10001, and LH11122.

[48] Masaki Fujimoto thanks the reviewers for their assistance in evaluating this manuscript.

## References

Agapitov, O., V. Krasnoselskikh, Y. Zaliznyak, V. Angelopoulos, O. Le Contel, and G. Rolland (2010), Chorus source region localization in

- the Earth’s outer magnetosphere using THEMIS measurements, *Ann. Geophys.*, **28**, 1377–1386.
- Burton, R. K., and R. E. Holzer (1974), The origin and propagation of chorus in the outer magnetosphere, *J. Geophys. Res.*, **79**, 1014–1023.
- Carpenter, D. L., and R. R. Anderson (1992), An ISEE/whistler model of equatorial electron density in the magnetosphere, *J. Geophys. Res.*, **97**, 1097–1108.
- Carpenter, D. L., M. A. Stasojevic, T. F. Bell, U. S. Inan, B. W. Reinisch, I. A. Galkin, R. F. Benson, J. L. Green, S. F. Fung, and S. A. Boardsen (2002), Small-scale field-aligned plasmaspheric density structures inferred from the Radio Plasma Imager on IMAGE, *J. Geophys. Res.*, **107**(A9), 1258, doi:10.1029/2001JA009199.
- Cornilleau-Wehrin, N., et al. (2003), First results obtained by the Cluster STAFF experiment, *Ann. Geophys.*, **21**, 437–456.
- Décrou, P. M. E., et al. (2001), Early results from the Whisper instrument on CLUSTER: an overview, *Ann. Geophys.*, **19**, 1241–1258.
- Dennis, J. E., Jr., and R. B. Schabel (1983), *Numerical Methods for Unconstrained Optimization and Nonlinear Equations*, Prentice-Hall, Upper Saddle River, N. J.
- Gurnett, D. A., R. R. Anderson, F. L. Scarf, R. W. Fredricks, and E. J. Smith (1979), Initial results from the ISEE 1 and 2 plasma wave investigation, *Space Sci. Rev.*, **23**, 103–122.
- Gurnett, D. A., et al. (2001), First results from the Cluster wideband plasma wave investigation, *Ann. Geophys.*, **19**, 1259–1272.
- Gustafsson, G., et al. (2001), First results of electric field and density observations by Cluster EFW based on initial months of operation, *Ann. Geophys.*, **19**, 1219–1240.
- Inan, U. S., M. Platino, T. F. Bell, D. A. Gurnett, and J. S. Pickett (2004), Cluster measurements of rapidly moving sources of ELF/VLF chorus, *J. Geophys. Res.*, **109**, A05214, doi:10.1029/2003JA010289.
- Hayakawa, M., K. Hattori, D. Lagoutte, M. Parrot, and F. Lefeuvre (1990), Direction finding of chorus emissions in the out magnetosphere and their generation and propagation, *Planet. Space Sci.*, **38**, 135–143.
- Helliwell, R. A. (1965), Whistlers and related ionospheric phenomena, 343 pp., Stanford Univ. Press, Stanford, Calif.
- Khotyainsev, Y., P.-A. Lindqvist, A. Eriksson, and M. André (2010), The EFW data in the CAA in *The Cluster Active Archive: Studying the Earth’s Space Plasma Environment*, edited by H. Laakso, M. G. T. T. Taylor, and C. P. Escoubet, pp. 97–108, Springer, Berlin.
- Nagano, I., S. Yagitani, H. Kojima, and H. Matsumoto (1996), Analysis of Wave Normal and Poynting Vectors of the Chorus Emissions Observed by GEOTAIL, *J. Geomag. Geoelectr.*, **48**, 299–307.
- Omura, Y., D. Nunn, H. Matsumoto, and M. J. Rycroft (1991), A review of observational, theoretical and numerical studies of VLF triggered emissions, *J. Atmos. Terr. Phys.*, **53**, 351–368.
- Parrot, M., O. Santolik, N. Cornilleau-Wehrin, M. Maksimovic, and C. Harvey (2003), Source location of chorus emissions observed by Cluster, *Ann. Geophys.*, **21**, 473–480.
- Pedersen, A., et al. (2008), Electron density estimations derived from spacecraft potential measurements on Cluster in tenuous plasma regions, *J. Geophys. Res.*, **113**, A07S33, doi:10.1029/2007JA012636.
- Rème, H., et al. (2001), First multispacecraft ion measurements in and near the Earth’s magnetosphere with the identical Cluster ion spectrometry (CIS) experiment, *Ann. Geophys.*, **19**, 1303–1354, doi:10.5194/angeo-19-1303-2001.
- Rytov, S. M., Y. A. Kravtsov, and V. I. Tatarskiy (1978), Introduction to the statistical radiophysics, *Moscow Sci.*, **2**, 463 pp.
- Santolik, O., and D. Gurnett (2003), Transverse dimensions of chorus in the source region, *Geophys. Res. Lett.*, **30**(2), 1031, doi:10.1029/2002GL016178.
- Santolik, O., D. A. Gurnett, and J. S. Pickett (2004), Multipoint investigation of the source region of storm-time chorus, *Ann. Geophys.*, **22**, 2555–2563.
- Santolik, O., D. A. Gurnett, J. S. Pickett, M. Parrot, and N. Cornilleau-Wehrin (2005), Central position of the source region of storm-time chorus, *Planet. Space Sci.*, **53**, 299–305.
- Sonwalkar, V. S. (2006), The influence of plasma density irregularities on whistler-mode wave propagation, *Lecture Notes Phys.*, **687**, 141–191.
- Sazhin, S. S., and M. Hayakawa (1992), Magnetospheric chorus emissions: A review, *Planet. Space Sci.*, **40**, 681–697.
- Tchernov, L. A. (1977), Waves in the randomly inhomogeneous medium, *Moscow Sci.*, 170 pp.
- Trakhtengerts, V. (1999), A generation mechanism for chorus emission, *Ann. Geophys.*, **17**, 95–100.
- Tsurutani, B. T., and E. J. Smith (1974), Postmidnight chorus: A substorm phenomenon, *J. Geophys. Res.*, **79**, 118–127.

Yagitani, S., I. Nagano, H. Matsumoto, Y. Omura, W. R. Paterson, L. A. Frank, and R. R. Anderson (1999), Wave and particle measurements for chorus emissions by GEOTAIL in the magnetosphere, *Adv. Space Res.*, 24, 91–94.

---

O. Agapitov, Astronomy and Space Physics Department, National Taras Shevchenko University of Kiev, Academic Glushkov Ave. 2, Kiev 03121, Ukraine. (agapit@univ.kiev.ua)

T. Dudok de Wit and V. Krasnoselskikh, LPC2E/CNRS, Universite d'Orleans, 3A Ave. de la Recherche Scientifique, Orleans F-45071, France.

Y. Khotyaintsev, Swedish Institute of Space Physics, Box 537, Uppsala SE-751 21, Sweden.

J. S. Pickett, Department of Physics and Astronomy, University of Iowa, Off. 715, Van Allen Hall, Iowa City, IA 52242, USA.

G. Rolland, CNES, 18 Ave. Edouard Belin, Toulouse CEDEX 4, F-31401, France.

O. Santolík, Faculty of Mathematics and Physics, Charles University, V Holesovickach 2, Prague 8 18000, Czech Republic.